Correlation between the Coarse- and Fine-Grained HAZ Hardness of X70 Pipeline SMA Welded Girth Welds

CGHAZ and FGHAZ hardness data from different SMAW passes were compared to determine their correlation

BY A. HINTZE CESARO, G. LEHNHOFF, AND E. WILLETT

Introduction

Analysis of recent pipeline girth weld failures, which have occurred predominantly in X70 pipeline girth welds using shielded metal arc welding (SMAW), has identified weld heat-affected zone (HAZ) softening as a possible contributing factor as it relates to low tensile strain capacity and strain localization at the girth welds (Refs. 1, 2). This finding has spurred interest in understanding the causes of HAZ softening.

Mohammadijoo et al. found that various changes in line pipe steel composition and welding parameters influenced the extent of HAZ softening (Ref. 3). Willett and Lehnhoff similarly observed that both pipeline material and weld heat input influenced HAZ softening (Ref. 4). Portella Garcia et al. showed that the absolute minimum hardness in pipeline weld HAZs is well-predicted by the P_{cm} carbon equivalent and weld cooling rate, but the HAZ softening relative to the base metal (BM) correlates poorly with P_{cm} because BM hardness is also strongly influenced by thermomechanically controlled processing history, not just P_{cm} (Ref. 5).

Portella Garcia et al. also reported the minimum HAZ hardness occurred within the fine-grained HAZ (FGHAZ) near the intercritical HAZ (ICHAZ) boundary (Ref. 5), which is in agreement with findings from Takahashi and Ogawa (Ref. 6), Hamada et al. (Ref. 7), and Li et al. (Ref. 8). Bang and Kim further showed that the minimum hardness in pipeline weld HAZs can be accurately predicted by considering austenite decomposition in the FGHAZ based on the composition, grain size, and weld cooling rate (Ref. 9).

It is worth noting that not all steel systems experience the minimum HAZ hardness at the lower temperature boundary of the FGHAZ, where the hardness is dominated by decomposition of FG austenite to higher-temperature, softer transformation products. Pisarski and Dolby reported HAZ softening can occur in the subcritical HAZ (SCHAZ), ICHAZ, and FGHAZ (Ref. 10). In pearlitic rail steel flash welds, Porcaro et al. found that the minimum HAZ hardness occurred at a lower relative temperature at the ICHAZ and SCHAZ boundary, where softening was also largely influenced by spheroidization of the existing pearlitic cementite (Ref. 11). Hanhold et al. showed that in quench and tempered martensitic steels, the minimum HAZ hardness can occur at even lower relative temperatures fully within the SCHAZ due to additional tempering of the existing tempered martensite structure (Ref. 12). Due to the differences in location and the mechanism of softening, the underlying factors affecting HAZ softening, and their potential mitigation strategies may differ between pipeline steels and other steel systems.

Within the pipeline welding literature, a large volume of research has also focused on limiting the maximum HAZ hardness, which occurs in the coarse-grained HAZ (CGHAZ). For example, high CGHAZ hardness has been historically related to poor toughness behavior and can contribute to hydrogen-assisted cold cracking (Ref. 13) or exceed limits for specific pipeline applications, such as sour service (Refs. 14, 15) or hydrogen gas service (Ref. 16). In the CGHAZ, high hardness is due to decomposition of CG austenite to lower-transformation products, such as bainite. Thus, control of the maximum hardness must consider the composition, grain size, and cooling rate of the CGHAZ (Ref. 17). These are the same considerations governing the minimum hardness experienced in the FGHAZ. As a result, a strong correlation between the minimum hardness and maximum hardness in pipeline welds is expected.

However, to the authors' knowledge, this correlation between CGHAZ and FGHAZ hardness has not been directly demonstrated in the literature. Mohammadijoo et al. generally observed that alloying approaches that increased the minimum hardness also increased the maximum hardness, which impaired impact toughness but did not quantify the
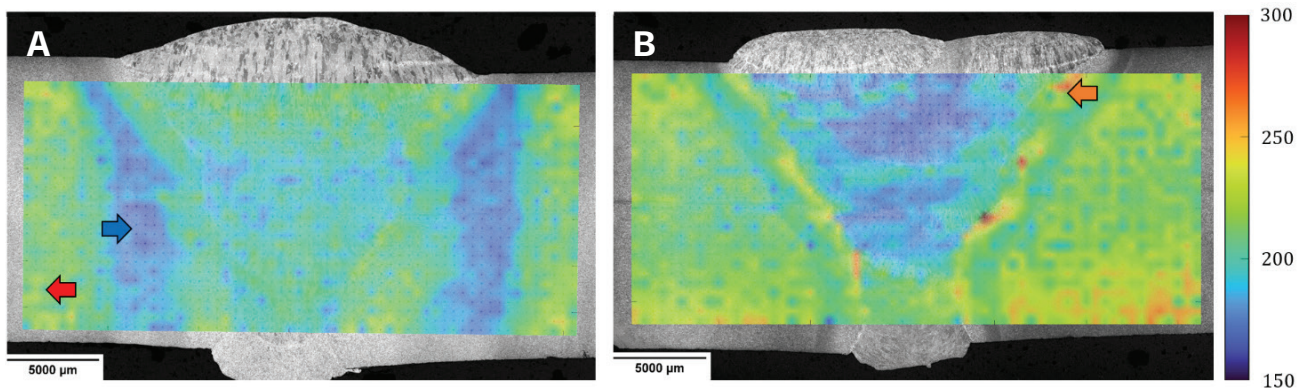
Fig. 1 — Macrographs and hardness (HV0.5) maps for material B welds: A — High heat input; B — low heat input. The arrows indicate the locations of the BM (red), FGHAZ (blue), and CGHAZ (orange) micrographs presented in Fig. 2.
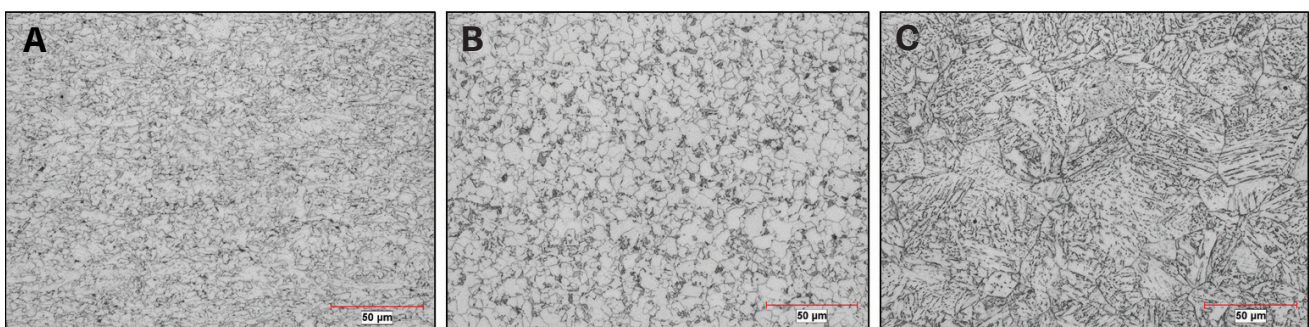

Fig. 2 — Example of optical micrographs for material B (as shown by the arrows in Fig. 1): A — BM (~ 217 HV); B — high-heat-input FGHAZ (~ 177 HV); C — low-heat-input CGHAZ (~ 237 HV).

Table 1 — Wall Thickness, P_{cm}, CEN, and Average BM Hardness for the Studied Materials

Material	WT (mm)	P_{cm}	CEN	BM HV
A (Ref. 4)	14.8 [0.582 in.]	0.142	0.208	211
B (Ref. 4)	15.2 [0.598 in.]	0.177	0.249	217
C (Ref. 3)	19 [0.748 in.]	0.166	0.234	221

5) and Hamada et al. (Ref. 7) observed a strong correlation between the minimum HAZ hardness and the P_{cm} as well as the maximum HAZ hardness and the P_{cm}, but they did not directly compare the minimum and maximum HAZ hardnesses (Refs. 5, 7). For deep-sea pipeline steel, Li et al. demonstrated that vanadium additions and reduced weld heat input increased the minimum weld HAZ hardness but also increased the maximum weld HAZ hardness (Ref. 8).

In this work, numerous X70 pipeline multipass SMA welded girth welds were characterized to confirm that the locations of minimum and maximum HAZ hardness occurred within the FGHAZ and CGHAZ zones, respectively. The CGHAZ and FGHAZ hardness data from different passes were also compared to determine the extent of their correlation. Finally, the implications of the correlation are demonstrated for applications that may require control of both the minimum and maximum HAZ hardness.

Table 2 — Weld Tests and Heat Input Ranges Per Pass

Material	Number of Welds	Heat Input Ranges (kJ/mm)			
		Root Pass	Second Pass	Intermediate Pass	Cover Pass
A	6	0.75–0.90	1.00–2.90	1.00–3.00	1.15–3.25
B	6	0.75–0.90	1.00–1.55	1.05–3.80	1.13–3.25
C	3	0.69–1.43	0.66–1.32	2.28–3.78	0.85–2.00

Experimental Procedures

Materials and Weld Experiments

A total of 15 welds performed in previous studies (Refs. 3, 4) on three different X70 materials were analyzed. The wall thickness (WT), P_{cm} and CEN carbon equivalent values, and average BM hardness of the studied materials are presented in Table 1. Within the studies, each weld was made with an intentionally different heat input and filler metal to keep the same interpass temperature of 100°C (212°F) for all welds. A summary of the test weld heat input range per pass is provided in Table 2. More information on the weld parameters can be found in Refs. 3 and 4.

Hardness Mapping

Cross-sectional hardness specimens were prepared by metallographic grinding and polishing to a 1-micron finish and then etching in 2% Nital. Vickers microhardness (HV) mapping was performed using 500 gram-force (gf) and a grid spacing of 0.5 mm (0.019 in.). For each specimen, the average BM hardness was calculated by averaging the hardness values from the two outermost columns of hardness indents (the entire WT) on both sides of the weld.

Each cross-sectional specimen was vertically divided into three different regions representing the cap, fill, and hot and root passes. As per AWS A3.0, *Standard Welding Terms and Definitions*, cap pass, fill pass, and hot pass will henceforth be referred to as cover pass, intermediate pass, and second pass, respectively. The hardness indent rows were manually assigned to the different passes using the etched weld cross section as a reference. The second and root passes could not be consistently differentiated due to the extent of the hardness grid, weld offset, and insufficient etching contrast. As a result, they were combined for the analysis. For each pass, the maximum hardness was determined by averaging
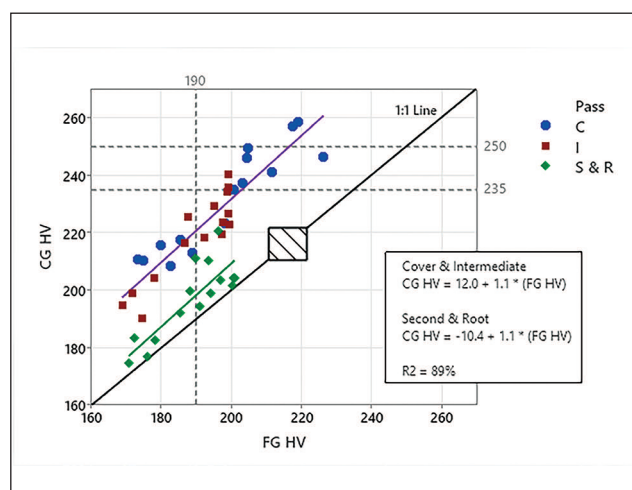

Fig. 3 — Hardness of the CGHAZ vs. FGHAZ for the cover, intermediate, and second and root passes.

the hardness values of the indents adjacent to the fusion line (i.e., in the CGHAZ), and the minimum hardness was calculated by averaging the softened points between the BM and the CGHAZ (i.e., in the FGHAZ).

Results and Discussion

Figure 1 shows the etched weld cross sections and the color indexed hardness maps of two different welds performed in material B with significantly different average heat inputs in all the passes (except for the root pass).

Figure 2 shows representative microstructures for regions of interest in material B. Figure 2A corresponds to the BM's microstructure composed of quasi-polygonal ferrite, acicular ferrite, and second phases. Figure 2B shows the microstructure from a region of minimum HAZ hardness in a high-heat-input intermediate pass composed of more-equiaxed ferrite grains and second phases. The micro-

structure is consistent with the FGHAZ and corroborates observations made by other authors that pipeline steels exhibit maximum HAZ softening in the FGHAZ (Refs. 5–9). Figure 2C shows the microstructure from a region of maximum HAZ hardness in a low-heat-input cover pass, which is consistent with the typical bainitic ferrite structure of the CGHAZ in these materials. Accordingly, the locations of minimum and maximum HAZ hardness will also be referred to as the FGHAZ and CGHAZ, respectively.

Figure 3 shows the average CGHAZ hardness vs. the average FGHAZ hardness for all welds separated by the root and second, intermediate, and cover passes. The black diagonal line represents a 1:1 line. Multiple linear regression was performed for the CGHAZ's hardness using the FGHAZ's hardness as a continuous variable and the welding pass as a categorical variable. The interaction term was not statistically significant, meaning that the slope for all passes should be assumed equal. Only the root and second pass data set showed a statistically different y-intercept, so the cover and intermediate passes were combined for the final regression model, which is included in Fig. 3. The R^2 value of 89% indicated that most of the observed variation in CGHAZ hardness could be explained by the pass it was generated from and its corresponding FGHAZ hardness, independent of the material and welding parameters used to make the weld.

Furthermore, a CGHAZ vs. a FGHAZ hardness slope of 1 would indicate that the two regions of the HAZ were responding identically to the underlying changes in composition and welding parameters contained in the data set. The regression slope was determined to be 1.1, which is very close to this theoretical value and supports the hypothesis that both the CGHAZ and FGHAZ are strongly influenced by a single mechanism, namely austenite decomposition kinetics. The difference in austenite grain size between the CGHAZ and FGHAZ was likely the primary cause of the different austenite decomposition products and resulting hardness in the two zones. Bulk alloying elements — such as manganese, silicon, and chromium — are expected to have similar hardenability effects within the two zones, and thus they are not expected to drastically influence the CGHAZ-FGHAZ hardness difference. The influence of microalloying elements — such as titanium, niobium, and vanadium — on the microstructure and hardness difference between the two zones may be more complex because microalloy precipitates may dissolve in the CGHAZ, allowing additional austenite grain coarsening compared to the FGHAZ. Furthermore, once in solution, microalloying elements can increase the austenite's hardenability and further influence the decomposition kinetics (Ref. 17).

The downward shift of the second and root pass regression line with respect to the cover and intermediate passes in Fig. 3 suggests that the final hardness of the HAZ from the first passes was also affected by the thermal cycle of subsequent passes through an annealing effect. Wang and Jia produced staggered root, second, intermediate, and cover pass SMA welds on X70 pipeline steel and observed similar softening of the root and second passes from the subsequent intermediate and cover passes (Ref. 2). However, it should be noted that softening and hardening of the HAZ with respect to the BM can occur through thickness, as depicted in Fig. 1.

Figure 3 contains additional annotations that illustrate how this type of combined CGHAZ and FGHAZ data can be utilized. The hashed rectangle on the 1:1 line represents the evaluated BM hardness range of 211–221 HV, as shown in Table 1. The vertical line at 190 HV represents FGHAZ softening to 90% of a BM hardness of 211 HV. Willett and Lehnhoff found that, if HAZ softening was maintained above approximately 89%, cross-weld tensile test specimens would not fracture in the HAZ, which serves as one metric for the tensile strain capacity of the HAZ (Ref. 4). Similarly, Wang and Jia recommended lower bound tensile strain capacity values as a function of the weld metal strength undermatching and the HAZ softening, where the critical thresholds in HAZ softening are ≤ 80%, ≤ 90%, or > 90% of the BM's hardness (Ref. 2). Thus, the 190 HV vertical line in Fig. 3 provides an estimated minimum HAZ hardness value above which HAZ softening is no longer expected to be a limiting factor for tensile strain capacity of the X70 welds included in this study.

The horizontal lines at 235 and 250 HV are the maximum weld HAZ hardnesses permitted for ASME B31.12 hydrogen gas service (Ref. 16) and CSA Z662 sour service (Ref. 14), respectively. For an X70 pipeline girth weld requiring a high tensile strain capacity from the FGHAZ and a maximum CGHAZ of 235 HV for ASME B31.12, the alloy design and welding procedure specification would need to promote CGHAZ-FGHAZ behavior that exists in the triangle formed between the 190 HV vertical line, the 235 HV horizontal line, and the diagonal 1:1 line. Similar reasoning would hold for CSA Z662, except that the 250 HV horizontal line would be used instead of the 235 HV horizontal line.

Of course, these examples are only illustrative because some hardness testing protocols for hydrogen gas and sour service do not use a full hardness grid pattern as was used in this study and instead require hardness testing at specific points (Refs. 15, 16). Regarding sour service, some standards allow wider hardness tolerances compared to CSA Z662. ISO 15156-2 (Ref. 15) similarly restricts hardness near the inside diameter (root/second passes) to 250 HV but allows up to 275 HV near the outside diameter (cover passes), which matches the natural tendency for the cover pass HAZs to have a higher hardness than the root and second passes.

Furthermore, standardized testing protocols and acceptance criteria for HAZ softening have not been adopted, so the vertical line at 190 HV cannot be interpreted as a firm boundary at this point. Slumkoski et al. proposed a methodology to test the HAZ softening susceptibility of a given steel, but the test uses only a single-pass bead-on-plate weld (Ref. 18) and likely cannot be used to set acceptance criteria because it does not include the influence of multiple passes (Ref. 2). It should also be reiterated that while the minimum hardness in the HAZ appears to be strongly influenced by austenite decomposition kinetics, the relative softening compared to the BM, and thus the effect on tensile strain capacity, will also be influenced by pipe strength, which is a function of chemistry and pipe thermomechanical history.

Nonetheless, the approach shown in Fig. 3 highlights the potential challenge of controlling both the minimum and maximum HAZ hardness simultaneously and suggests that future pipeline weld HAZ studies should consider both hard and soft HAZs since both can be important to weld performance and

both tend to be correlated with one another. Such studies may also help identify strategies to decouple the minimum and maximum HAZ hardness values in pipeline steels.

Conclusions

This study of weld HAZ hardness and microstructure in X70 pipeline multipass SMA welded girth welds revealed the following:

1) The hardest regions of the HAZ corresponded to the CG region, where the large austenite grain size from the welding heat input delayed austenite decomposition and promoted harder bainitic structures.

2) The softest regions of the HAZ corresponded to the FG region, where the small austenite grain size promoted austenite decomposition to softer equiaxed ferrite microstructures.

3) Conclusions 1 and 2 suggest that the minimum hardness (FGHAZ) and maximum hardness (CGHAZ) areas of the HAZ should be strongly correlated because they are both influenced by austenite decomposition kinetics. The CGHAZ and FGHAZ are indeed strongly correlated.

4) The hardness results also suggest that earlier passes are annealed by subsequent passes, leading to lower hardness near the inside diameter.

5) Pipeline applications requiring harder FGHAZs (minimal HAZ softening) for tensile strain capacity and softer CGHAZs for service environment compatibility (such as sour service or hydrogen gas service) will require careful selection of materials and welding parameters to balance the apparently conflicting requirements.

6) Because HAZ hardening and softening appear strongly correlated, future studies should consider both aspects simultaneously when possible.

References

1. Wang, Y. Y., Jia, D., Warman, D., Johnson, D. L., and Rapp, S. 2020. Improved linepipe specifications and welding practice for resilient pipelines. *Proceedings of the 13th International Pipeline Conference*. New York City, N.Y.: ASME. DOI: 10.1115/IPC2020-9725

2. Wang, Y. Y., and Jia, D. 2022. Guidance on the use, specification, and anomaly assessment of modern linepipes. *PRCI Project MATH-5-3B Report*. Chantilly, Va.: Pipeline Research Council.

3. Mohammadijoo, M., Collins, L., Rashid, M., and Arafin, M. 2020. Influence of steel chemistry and field girth welding procedure on performance of API X70 line pipe steels. *Proceedings of the 13th International Pipeline Conference*. New York City, N.Y.: ASME. DOI: 10.1115/IPC2020-9721

4. Willett, E., and Lehnhoff, G. 2022. Factors affecting SMAW pipeline girth weld strength and strain concentration under tensile loading. *Proceedings of the 14th International Pipeline Conference*. New York City, N.Y.: ASME. DOI: 10.1115/IPC2022-86735

5. Portella Garcia, M., Gervasyev, A., Lu, C., and Barbaro, F. J. 2022. Chemical composition and weld cooling time effects on heat-affected zone hardness of line pipe steels. *International Journal of Pressure Vessels and Piping* 200: 104837. DOI: 10.1016/j.ijpvp.2022.104837

6. Takahashi, A., and Ogawa, H. 1995. Influence of softened heat-affected zone on stress oriented hydrogen induced cracking of a high strength line pipe steel. *ISIJ international* 35(10): 1190–1195.

7. Hamada, M., Hirata, H., Okaguchi, S., Shitamoto, H., Yamamoto, A., Takahashi, N., Miura, M., and Takeuchi, I. 2008. Material design for line pipe steel to minimize HAZ softening and obtain good HAZ toughness. *International Journal of Offshore and Polar Engineering* 18(3): 204–210.

8. Li, B., Liu, Q., Jia, S., Ren, Y., and Yang, P. 2022. Effect of V content and heat input on HAZ softening of deep-sea pipeline steel. *Materials* 15(3): 794. DOI: 10.3390/ma15030794

9. Bang, K. S., and Kim, W. Y. 2002. Estimation and prediction of HAZ softening in thermomechanically controlled-rolled and accelerated-cooled steel. *Welding Journal* 81(8): 174-s to 179-s.

10. Pisarski, H. G., and Dolby, R. E. 2003. The significance of softened HAZs in high strength structural steels. *Welding in the World* 47(5): 32–40.

11. Porcaro, R. R., Faria, G. L., Godefroid, L. B., Apolonio, G. R., Cândido, L. C., and Pinto, E. S. 2019. Microstructure and mechanical properties of a flash butt welded pearlitic rail. *Journal of Materials Processing Technology* 270: 20–27. DOI: 10.1016/j.jmatprotec.2019.02.013

12. Hanhold, B., Babu, S. S., and Cola, G. 2013. Investigation of heat affected zone softening in armour steels: Part 1 — Phase transformation kinetics. *Science and Technology of Welding and Joining* 18(3): 247–252. DOI: 10.1179/1362171812Y.0000000100

13. Lippold, J. C. 2015. *Welding Metallurgy and Weldability*. Hoboken, N.J.: John Wiley & Sons Inc.

14. CSA Z662:19, *Oil and gas pipeline systems*. 2019. Toronto, Ontario: CSA Group.

15. ISO 15156-2:2020(E), *Petroleum and natural gas industries — Materials for use in H$_2$S-containing environments in oil and gas production — Part 2: Cracking-resistant carbon and low-alloy steels, and the use of cast irons*. 2020. Fourth Edition. Switzerland: ISO.

16. ASME B31.12-2019, *Hydrogen Piping and Pipelines*. 2019. ASME: New York, N.Y.

17. Robinson, I. D. G. 2016. Grain growth and austenite decomposition in two niobium containing high strength line pipe steels. Master's thesis. British Columbia, Canada: The University of British Columbia.

18. Slumkoski, Z., Dinovitzer, A., Begg, D., and Guest, S. 2022. Heat affected zone softening susceptibility test development. *PRCI Project MATH-5-3C Report*. Chantilly, Va.: Pipeline Research Council.

ALEJANDRO HINTZE CESARO (*alejandro.hintzecesaro@ evrazna.com*) and **GREG LEHNHOFF** are with EVRAZ North America, Saskatchewan, Canada. **ERIC WILLETT** is with TC Energy, Alberta, Canada.